QTG Quadrupole Magnets for the CNGS Transfer Line

D. Cornuet, O. Kiselev, E. Levichev, O. Pavlov, Y. Pupkov, E. Ruvinsky, and T. Zickler

***Abstract*—The QTG quadrupole magnets will be a part of the CERN Neutrino to Gran Sasso (CNGS) transfer line. 23 QTG magnets will be used as lattice and matching quadrupoles. They are being produced in the framework of a German in-kind contribution via DESY to CNGS. The QTG magnets have a maximum gradient of 40 T/m at the 530 A excitation current and are manufactured from laminated steel cores. The yoke length is 2.2 m and the inscribed radius is 22.5 mm. The excitation coils are made of vacuum impregnated hollow copper conductor. The main design aspects and the results of the acceptance tests including mechanical, electrical and magnetic field measurements are described.**

***Index Terms*—Accelerator magnets, magnetic analysis, magnetic field measurements, proton beams.**

I. Introduction

THE CERN neutrino to Gran Sasso (CNGS) project, presently under construction, is a collaboration between CERN and the Gran Sasso Laboratory in Italy to study neutrino oscillations in a 730 km long base line experiment. A primary beam line TT41, about 830 m long, will be built to transfer protons at 400–450 GeV from SPS to the target. The TT41 line will be equipped with conventional magnets including 23 QTG type quadrupoles.

The QTG quadrupole magnets, which will be used to focus the proton beam, have the same cross-section and magnetic length but different excitation currents. The main parameters of the QTG magnets are listed in Table I.

TABLE I
Main Parameters of the QTG Magnets

Parameter	Value	Unit
Number of magnets	23	
Operating gradient range	From 12.4 to 30.2	T/m
Maximum gradient	40	T/m
Inscribed radius	22.5	mm
Good field region	r ≤ 21	mm
Gradient integral quality	$\leq \pm 2 \times 10^{-3}$ (x,y ≤ 21 mm)	
$\Delta\int$Gdl / $\int$Gdl	$\leq \pm 3 \times 10^{-3}$ (21 ≤ x,y ≤ 27 mm)	
Yoke length	2200	mm
Maximum current	530	A
Resistance at 20 °C	51.4	mΩ

II. Magnet Design and Fabrication

A. Magnet Design

A schematic cross sectional view of the magnet with flux lines is shown in Fig. 1. According to the 2D simulation a maximum saturation of about 1.7 T is reached inside the iron pole.

The hyperbolic pole contour was optimized using the ANSYS finite element code [1] and cross-checked by the program MERMAID [2] developed at BINP. A contour was obtained that provides a relative central gradient quality of $\Delta G/G_0 < \pm 10^{-3}$ inside the good field region for all levels of working gradients. The partial gradient errors defined as

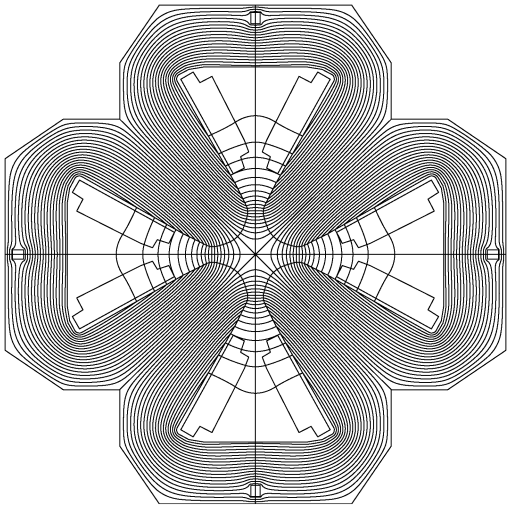

Fig. 1. QTG magnet cross section.

$$B_Y = \sum_{n=1}^{18} (B_n \cos(n-1)\theta - A_n \sin(n-1)\theta) \cdot r^{n-1} \quad (1)$$

$$\frac{\Delta G(r)}{G_0} = B_2^{-1} \sum_{n=3}^{N} (n-1) \cdot (B_n + iA_n) \cdot \left(\frac{r}{R_r}\right)^{n-2} \quad (2)$$

at the radius $R_r = r = 21$ mm for the maximum gradient (40 T/m) and nominal gradient (26.7 T/m) are listed in Table II.

One can see that the 10th harmonic multipole component gives the major contribution to the 2D gradient error. It is well known that the integrated field quality can be improved by the end-pole chamfer. The configuration of the chamfer was carefully studied with the help of the 3D MERMAID module. Different shapes and sizes were checked. The dependence of the

Manuscript received October 20, 2003.

D. Cornuet is with CERN, CH-1211, Geneva 23, Switzerland (e-mail: didier.cornuet@cern.ch).

O. Kiselev, E. Levichev, O. Pavlov, Y. Pupkov, and E. Ruvinsky are with Budker Institute of Nuclear Physics (BINP), 630090, Novosibirsk, Russia.

T. Zickler is with CERN, CH-1211, Geneva 23, Switzerland (e-mail: thomas.zickler@cern.ch).

Digital Object Identifier 10.1109/TASC.2004.829985

TABLE II
PARTIAL GRADIENT ERROR

	$(\Delta G_n / G_0) \times 10^3$	$(\Delta G_n / G_0) \times 10^3$
G_0	nom	max
$n = 6$	0.2072	-0.0725
$n = 10$	0.3506	0.2894
$n = 14$	0.00063	-0.00024
$n = 18$	-0.00013	-0.00124

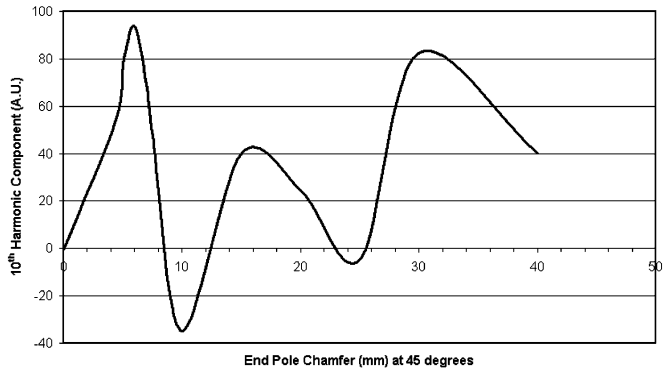

Fig. 2. The value of the 10th 3D-harmonic of the QTG gradient as a function of the end pole chamfer size.

10th harmonic on the chamfer size for the cut angle of 45° is depicted in Fig. 2.

With the help of the 3D magnetic field simulation the shape and size of the end pole chamfers were chosen to satisfy the requirements for the integrated gradient quality. The magnetic length of the magnet is also a function of the end pole chamfers. Fig. 3 shows the deviation of

$$\Delta L_{\frac{1}{2}} = \frac{(L_m - L_y)}{2}$$

versus the size of the 45°-pole tip cut (here $L_{\rm m}$ and L_y are the magnetic and yoke length, respectively). The two effective length curves were calculated from (a) the integrated harmonic analysis and (b) the integrated field calculation. In such a way the results have been cross-checked using the MERMAID simulation code.

B. Fabrication

Fig. 4 shows the QTG quadrupole magnet mounted on the magnetic measurement stand. The magnet is assembled from four quadrants each with a pre-assembled excitation coil. The cores are made from precisely punched 1.0-mm thick laminations held together by welded end plates and angular plates. The punching accuracy for the pole profile and the reference edges of the lamination is ± 20 μm. Laminations are stacked in a rigid frame and compressed between two 30 mm thick end plates made of annealed low-carbon steel. The packing factor is larger than 97%.

The 16-turn excitation coil is wound from one continuous piece of hollow copper conductor in two layers. The oxygen-free copper conductor has a square cross section of 11 mm $\times$ 11 mm. The conductor is insulated with glass cloth tape and impregnated with radiation resistance epoxy resin.

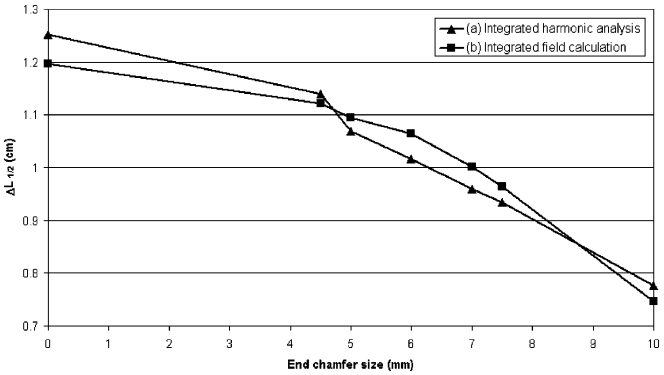

Fig. 3. QTG effective length as a function of the end pole chamfer size.

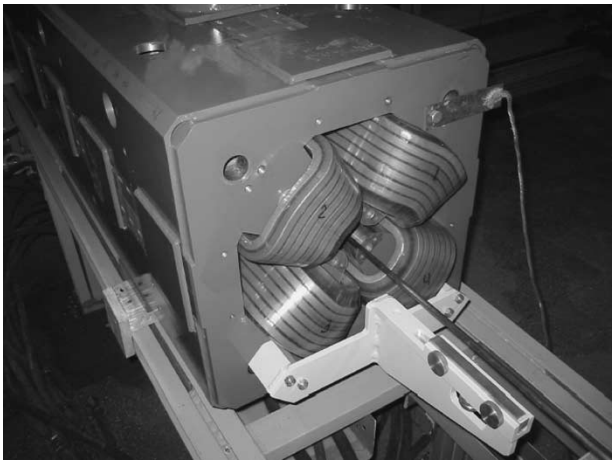

Fig. 4. First QTG magnet on the magnetic measurement bench at BINP.

III. PROTOTYPE MAGNETIC MEASUREMENTS AT BINP

The first QTG quadrupole magnet has been manufactured and tested mechanically, electrically and hydraulically at BINP. Magnetic measurements have been performed with an array of 14 Hall probes. The probes have a 5 mm horizontal spacing and provide a measurement range of ± 32.5 mm. The copper plate holding the Hall probe array is equipped with a temperature sensor to compensate the field measurements for any temperature variation of the Hall probes. The array is moved by a step motor along the quadrupole axis with an accuracy of about 0.1 mm.

Two measurements are required to get a gradient map in one of the transverse planes. During the first run, the whole probe array is shifted by 2.5 mm to the left of the magnet center, whereas during the second run the array is shifted by 2.5 mm to the right. As a result, the same probe measures two adjacent transversal positions. This technique allows to eliminate systematic errors of individual probes. Before starting the series measurements, the Hall probes are calibrated using a dipole magnet which provides a homogeneous field quality and NMR probes giving the absolute field value. The field mapping is preceded by four magnetization cycles from 0 to 450 A at a rate of 25 A/s.

The excitation curve has been measured at 10 different currents. At the nominal current of 340 A the saturation is 2%, while at the maximum current of 500 A it is 3.8%.

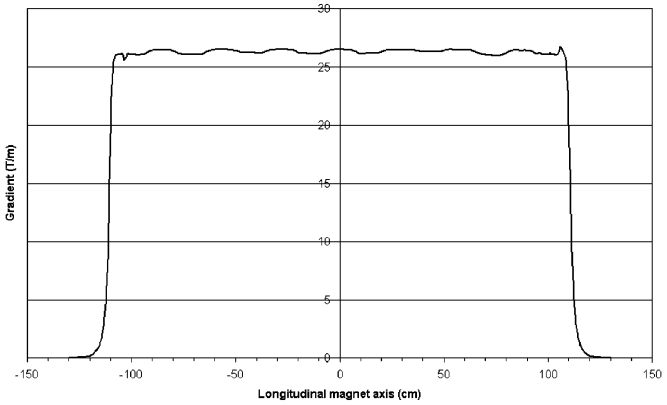

Fig. 5. Longitudinal modulation of the QTG gradient at 340 A.

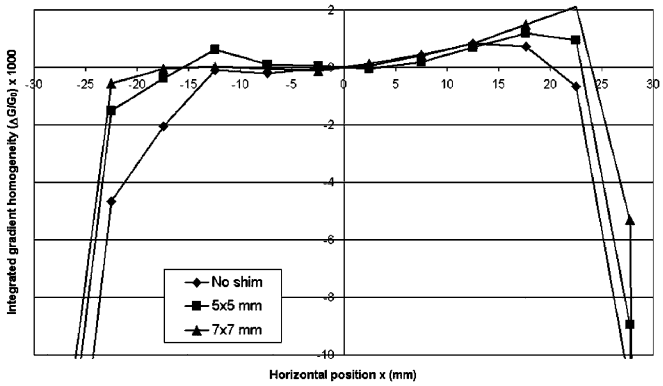

Fig. 6. Optimization of the QTG integrated gradient in the horizontal plane by the end pole bevel.

The long QTG magnet with a relatively small cross section area is sensitive to assembly tolerances and the gradient shows strong regular undulation in the direction of the longitudinal magnet axis (see Fig. 5).

The period of this undulation corresponds to the position of the fixing tie plates, which hold the magnet quadrants together. Mechanical measurements of the distance between the four poles gave similar results (see below). When the gradient measurement shows the maximum, the minimum distance between two adjacent poles was observed. The most likely explanation for this effect could be the deformation of the quadrants due to stress induced by welding the quadrants together. This deformation also results in the large difference in the gradient homogeneity at the location of the fixing plates and between them. In other words, the gradient quality also undulates along the magnet axis.

To improve the quality of the integrated gradient and to reach the values indicated in Table I, a 45-degree chamfer was applied on each tip of the quadrant poles. Earlier, this technique was used successfully for the MQI quadrupole magnet for the LHC transfer lines [3]. The results of the magnet shimming are shown in Fig. 6 (for the horizontal mapping) and in Fig. 7 (for the vertical mapping).

One can see a significant improvement of the integral gradient homogeneity in the region between ± 15 and 23 mm. For the

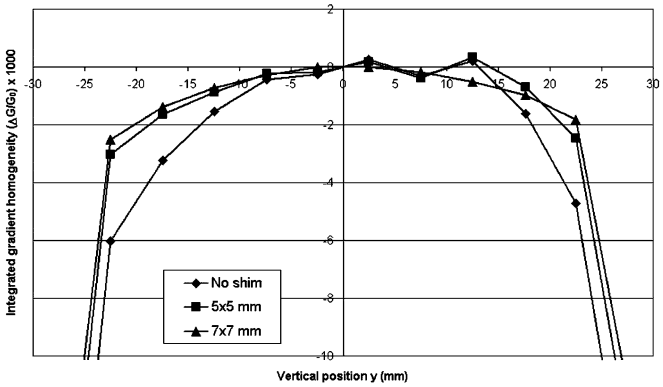

Fig. 7. Optimization of the QTG integrated gradient in the vertical plane by the end pole bevel.

TABLE III
COMPARISON OF THE COEFFICIENT $k(x)$ FROM (4)

x (mm)	k_{exp}	k_{sim}
17	0.18	0.17
22	0.45	0.42
27	0.72	0.72

prototype of the QTG magnet a chamfer of $45^\circ \times 10$ mm was chosen, providing a homogeneity the integrated gradient of

$$\delta_x = (0.8 \ldots 1.0) \times 10^{-3}, \quad \delta_y = (-2.1 \ldots -1.0) \times 10^{-3},$$

inside the region $x, y = \pm 22.5$ mm. The definition of δ is

$$\delta_{x,y} = \frac{\left(\int G(s)ds\right)_{x,y} - \left(\int G(s)ds\right)_{x,y=0}}{\left(\int G(s)ds\right)_{x,y=0}}. \tag{3}$$

Another interesting aspect during the end pole shimming procedure was the ability to predict the 3D field configuration for the quadrupole magnets. Assuming the linear dependence of the integrated gradient correction on the shim size $45^\circ \times \Delta L$ mm (where ΔL varies from 3 mm to 10 mm)

$$\delta(x) = \delta(0) + k(x)\Delta L, \tag{4}$$

the following estimation of the coefficient $k(x)$ can be extracted from the measurement and the simulation.

The agreement between the experimental and calculated results shown in Table III seems quite good.

IV. MECHANICAL MEASUREMENTS AT CERN

The assembly tolerances inside the QTG prototype were verified with a Pole Distance Measurement Device (PDMD) [4]. The PDMD measures the deviation of the distances between two adjacent poles from their nominal value (13.748 mm) and the horizontal and vertical tilts of the gaps at 45 mm intervals along the aperture. The deviation of the pole distances is shown in Fig. 8. Maximum positive deviations (i.e., distance too large) of more than 600 μm have been measured on the positions of the welded tie plates, whereas the minima have been localized between the plates. These measurement results are in accordance with the magnetic measurements showing a field undulation along the magnet axis.

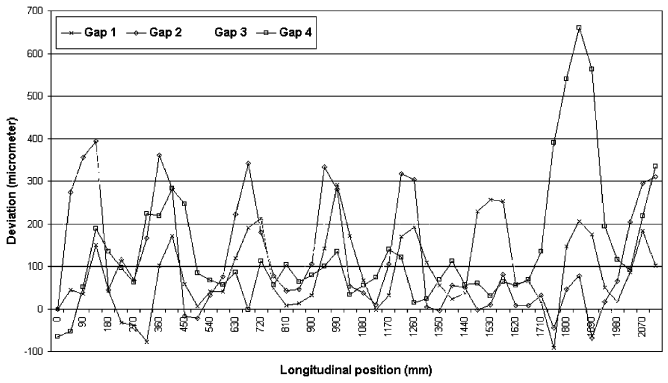

Fig. 8. Deviation of the distances between the poles measured with the PDMD.

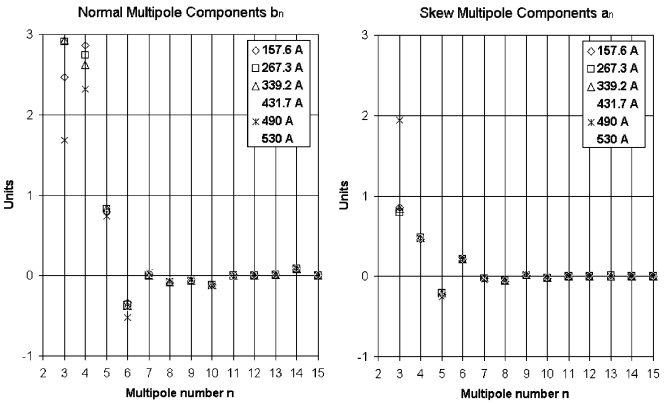

Fig. 9. Normal and skew harmonic multipole components of the QTG prototype measured at different currents.

V. Rotating Coil Measurements at CERN

After delivering the pre-series magnet to CERN the magnetic field was measured using a rotating coil mole. The mole has an outer diameter of 42 mm and an effective length of 750 mm. It was positioned in the aperture with the help of a 5-meter stainless steel support tube (316L grade). The mole contains 5 harmonic coils. The first coil gave the absolute signal, while the bucked combination of four coils gives the compensated signal in such a way that the main component (quadrupole) as well as the dipole component were suppressed. Before the magnetic measurement campaign, the magnet has been demagnetized by five cycles from 0 to 530 A with a rate of 100 A/s.

The mole measurements were done at four longitudinal positions; two were inside the magnet symmetrically around the center of the yoke and two were positioned to include the complete end fields. The integrated gradient and the integral harmonics were obtained from the sum of the four positions. Measurements at the position, midway along the magnet length, were used to obtain the field dependence on the excitation current and to get higher accuracy for the calculation of the equivalent length of the quadrupole.

The measurements were analyzed to obtain the multipole decomposition of the field at a reference radius R_r, relative to the main field component $B_N^{(r)}$ [5]. The multipole coefficients b_n and a_n represent the normal respectively the skew relative field errors at the reference radius. They are dimensionless and for practical reasons they are given in units of 10^{-4}. For this analysis n was limited to 15:

$$B_y + iB_x = B_2^{(r)} \cdot 10^{-4} \sum_{n=1}^{15} (b_n + ia_n) \left(\frac{z}{R_r} \right)^{n-1}. \quad (5)$$

Fig. 9 gives the measurement results with the integral harmonics expressed in normalized units. The natural harmonics 6, 10 and 14 are small (lower than 0.6 units even at the maximum current) which proves the good design of the magnet. On the other hand several units are measured for the sub-harmonics, which denote mechanical errors in the assembly of the quadrants.

TABLE IV
Equivalent Length of the QTG Quadrupoles

Current (A)	267.3	339.2	431.7	490	530
Equivalent length L_m(m)	2.210	2.209	2.207	2.204	2.201

The equivalent length $\mathrm{L_m}$ given in Table IV was computed by summing up the integral of the main field at the four measurement positions divided by the field at the central position and corrected by the gap created by the different displacements of the mole.

VI. Conclusion and Plans

The magnetic measurements done at CERN confirm the results from the measurements already undertaken at BINP and the characteristics expected in the design report. The sub-harmonics measured ($n = 3$, 4 and 5) confirm some mechanical errors after the assembly of the prototype magnet. These errors are also in accordance with the mechanical measurement results. To eliminate the deformation of the yoke due to welding the design of the tie side plates and the welding procedure has already been modified. Also a special tool is developed that will allow to increase assembling tolerance.

References

[1] T. Zickler, "Design Report of the QTG Quadrupoles for the CERN CNGS Line," CERN, SL-Note-2000-049 MS, September 2000.
[2] A. Dubrovin, *MERMAID User's Guide* Novosibirsk, 1994.
[3] K. M. Schirm *et al.*, "The quadrupole magnets for the LHC injection transfer lines," *IEEE Trans. Appl. Supercond.*, vol. 10, no. 1, pp. 154–157, March 2000.
[4] G. S. Clark, O. Hans, G. de Rijk, and M. Racine, "A twin aperture resistive quadrupole for the LHC," *IEEE Trans. Appl. Supercond.*, vol. 10, no. 1, pp. 147–149, March 2000.
[5] "Engineering Spec.,", LHC-MMS/ES01, LHC-M-ES-0001.00 rev.1.1.